Automatic generation control analysis of power system with nonlinearities and electric vehicle aggregators with time-varying delay implementing a novel control strategy

Nimai Charan PATEL[1][*] ![ORCID], **Binod Kumar SAHU**[2], **Manoj Kumar DEBNATH**[2]

[1]Department of Electrical Engineering, Government College of Engineering, Keonjhar, Odisha, India

[2]Department of Electrical Engineering, Siksha 'O' Anusandhan University, Bhubaneaswar, Odisha, India

Abstract: Automatic generation control (AGC) also known as load frequency control plays a vital role in interconnected power system for frequency regulation. Electric vehicles (EVs) with battery as the storage device can participate in frequency regulation service. In practice, a large number of EVs are aggregated as a single unit called EV aggregator for participation in frequency regulation service in AGC system. Participation of EV aggregators in AGC system for frequency regulation will be encouraged in near future because EVs have less environmental pollution than the conventional vehicles. However, participation of EV aggregators in AGC system may introduce time delay which degrades the dynamic performance of the power system and even may lead to system instability. Further, generation rate constraint (GRC) and governor dead band (GDB) of synchronous generator introduce nonlinearity in the system, which adversely affects its dynamic performance. Hence, selection of an appropriate control strategy is essential for performance enrichment of the power system. In this work, a PID-fuzzy-PID (PID-FPID) controller optimally designed by hybridizing particle swarm optimization (PSO) and modified sine cosine algorithm (MSCA) is proposed and a novel attempt is made to improve the frequency stability of a two-equal-area interconnected thermal power system with GDB and GRC incorporating an EV aggregators with time-varying delay in each area. Integral time absolute error has been chosen as the objective function to optimally design the controller parameters. Dynamic performance of the system is also investigated with proportional-integral-derivative (PID) controller optimally designed by PSO, sine cosine algorithm (SCA), MSCA, and hybrid PSO-MSCA. The efficacy and supremacy of the proposed hybrid PSO-MSCA-based PID-FPID control strategy is established by contrasting the results with the others. Finally, the robustness of the proposed control strategy is validated by (i) including two EV aggregators with time-varying delay in each area, (ii) applying a large disturbance of 0.4 p.u. in area-1, and (iii) applying a random load in area-1.

Key words: Automatic generation control, electric vehicle aggregators, time-varying delay, particle swarm optimization, modified sine cosine algorithm

1. Introduction

The use of electric vehicles (EVs) has been encouraged in recent years due to environmental issues and gradual depletion of fossil fuels. With the rapid increase of petroleum price and ever-growing global climate change causing acute environmental problems, researchers have found EVs to be the alternative energy solution for automobiles. With vehicle to grid (V2G) technology [1], large-scale integration of EVs is possible in modern interconnected power system. As a new type of load, EVs are likely to have several applications in V2G

---

[*]Correspondence: ncpatel.iter@gmail.com

technology: boosting the intermittent renewable energy sources usage without any compromise in robustness of operation to dynamic performance of the power system in the presence of renewable energy sources to the grid [2], promoting ancillary services [3] and so on. Frequency regulation with EVs is an important ancillary service [4, 5], which has found wide application in modern power system. EV owners participating in frequency regulation service avail the added advantage of income source from frequency regulation markets as reported in some studies [6–9]. Therefore, it is expected that EVs will play an important role in frequency regulation service in near future.

An outline of the concept regarding integration of EVs into the power system covering the technical as well as electricity market along with its effects and advantages was presented in [10], whereas frequency regulation by use of EV and V2G system was demonstrated in [11]. Practically for participation in frequency regulation service, a large number of EVs are aggregated as a unit called as EV aggregator [9, 12] to achieve a minimum regulation capacity. Effective automatic generation control (AGC) scheme should be implemented in power system with EV aggregators for quickly restoring the frequency and tie-line power at their nominal values. For AGC system, control signals are transferred to various EVs in EV aggregators through open communication channel. However, the time-varying delays caused by open communication channel may affect the stability of power systems. Many research works on stability analysis of time-delayed load frequency control (LFC) system considering various issues have been published in the literature. Design of a robust PID controller for LFC with time delay was presented in [13]. Computation of delay margin for time-delayed LFC system has been illustrated in the literature [14–16]. A gain scheduling method has been proposed for secondary frequency control with time delay [17]. Event triggering algorithm for stability of LFC of power system with communication delay has been presented in [18].

It is important to a design suitable controller in interconnected power systems to address the effect of time-varying delayed responses of EVs on the stability of AGC systems, when EV aggregators participate in the AGC systems. In addition, the controller gains could be optimized using various evolutionary algorithms to obtain superior dynamic performance of the AGC system. However, no studies have been reported in the literature regarding adoption of appropriate control strategy for load frequency control systems with EV aggregators having either constant or time-varying delays. In this work, a PID-fuzzy-PID (PID-FPID) controller optimally designed by hybridizing particle swarm optimization (PSO) and modified sine cosine algorithm (MSCA) is proposed for AGC of two-equal-area interconnected reheat thermal power system in the presence of an EV aggregator in both areas. To make the system more realistic, a thermal power system with generation rate constraint (GRC) and governor dead band (GDB) is considered and EV aggregator with time-varying delay is incorporated. Taking integral time absolute error (ITAE) as the objective function, when the system is subjected to a step load perturbation (SLP) of 10% in area 1, the dynamic response of the system is studied separately with two separate controllers, proportional integral derivative (PID) and PID-FPID controllers. The gains of the PID controllers are optimized using particle swarm optimization (PSO), sine cosine algorithm (SCA), modified sine cosine (MSCA) algorithm, and hybrid PSO-MSCA. Parameters of the PID-FPID controllers are optimized using hybrid PSO-MSCA to study the dynamic behavior of the system. A PSO optimized integral controller has been taken as the base case to study and compare the dynamic response of the system with the control strategies above. It was found that the PID-FPID controllers tuned with hybrid PSO-MSCA yields superior dynamic performance compared to the other controllers. Salient contributions of this research work are as follows:

    i. Modelling of a two-equal-area interconnected power system with each area consisting of a thermal generating unit and an EV aggregator with time-varying delay.

    ii. Modification of SCA to develop MSCA and hybridization of PSO and MSCA.

    iii. Optimal design of conventional PID controller through PSO, SCA, MSCA, and hybrid PSO-MSCA.

    iv. Optimal design of PID-FPID controller employing hybrid PSO-MSCA.

    v. Performance comparison of the results and convergence profile analysis to demonstrate the superiority of the proposed control strategy over the others.

    vi. Validation of the robustness of the proposed control strategy.

2. System modelling

EV aggregators participate in frequency regulation service when a large number of EVs stand in a parking area. When EV aggregators participate in frequency regulation service, they receive the command for regulation of power from the load center and the same is allocated and transferred to each participating EV with communication delay. Hence, EV aggregator exhibits time delay response which deteriorates the dynamic performance of the AGC system and it may even cause system instability.

2.1. EV aggregator with time-varying delay

A large number of EVs are considered as a unit known as EV aggregator where each EV has a delay component. Assuming that the EVs of the EV aggregator do not have either full state-of-charge battery or empty state-of-charge battery, the input–output relationship of the battery system of an EV can be represented by the 1st order transfer function as given below in Eq. (1): [19–21].

$$G_{EV}(s) = \frac{\Delta P_{EV}(s)}{\Delta P_C(s)} = \frac{K_{EV}}{1 + sT_{EV}},\tag{1}$$

where ΔP_{EV} represents the incremental changes in output power of EV aggregator, ΔP_C represents the control input to the EV aggregator, K_{EV} is the gain, and T_{EV} is the time constant of the battery system of EV aggregator. The communication delay that takes place when transferring the control signal from EV aggregator to EV and scheduling delay of EV aggregator is modelled by considering an exponential transfer function $e^{-s\tau(t)}$. For easy analysis, it is assumed that the time delay and time constant T_{EV} for each EV is same. With this assumption, the transfer function model of the EV aggregator is obtained as given above in Eq. (1).

A sine wave function is used to mathematically model the time-varying delay. Both the amplitude and bias of the sine function are taken as 1. A literature review reveals that for time-varying delay systems, the first derivative value of the time-varying delay should not exceed the unity; otherwise, the system stability could not be maintained [22]. Hence, to maintain the system stability and to improve system performance, the following constraint as given in Eq. (2) should be implemented [23, 24].

$$\frac{d\tau(t)}{dt} \leq 1.\tag{2}$$

This restriction has been imposed in this work while modelling the power system under consideration; therefore, the angular frequency ω in the sine function is taken as 1 rad/sec so that the 1st delay derivative is always

restricted to be less than or equal to 1. Furthermore, each EV aggregator has a time-varying delay within the range [0,5] s.

2.2. LFC model including EV aggregators with time-varying delay

Transfer function model of the two-equal-area interconnected power system under study is shown in Figure 1. Each area of the power system consists of a thermal unit with GDB, reheat turbine, GRC, and an EV aggregator with time-varying delay. Generation rate of the thermal unit is restricted by adding limiters in the system. In the model, GRC of 3%/min is taken for each thermal unit by using two limiters to restrict the generation rate. Furthermore, mechanical friction and backlash valve overlaps in hydraulic relays cause the governor dead-band. It has the effect that for a given position of the governor control valves, there can be an increase/decrease in speed before the position of the valve changes. The effect of GDB has also been included in the designed model. The limiting value of dead-band is specified as 0.036. Inclusion of GDB and GRC in the model introduces nonlinearities in the system.

LFC is based upon tie-line bias control, where there is a tendency of each area to reduce its area control error(ACE) to zero. ACE for each area is the linear combination of frequency and tie-line error. ACEs of each area is input to the controller of the corresponding area. The controller output of each area is given to the reheat steam plant and EV aggregator of the respective area. ACEs for the two area system are:

$$ACE_1 = \Delta P_{12} + B_1 \Delta \omega_1, \tag{3}$$

$$ACE_2 = \Delta P_{21} + B_2 \Delta \omega_2, \tag{4}$$

where $\triangle P_{12}$ and $\triangle P_{21}$ are tie-line power flow from area-1 to area-2 and from area-2 to area-1 respectively, B_1 and B_2 are bias factors of area-1 and area-2 respectively, $\triangle \omega_1$ and $\triangle \omega_2$ are frequency deviations in area-1 and area-2 respectively. ACEs are used as actuating signals to bring $\triangle \omega_1$, $\triangle \omega_2$, and $\triangle P_{tie}$ to zero when steady state is reached. Here α_1 and α_2 are the participation ratio of the steam generator and EV aggregator respectively. Parameters of the model considered in this work are taken from [16] and given in the appendix.

3. Controller structure
3.1. PID controller
Three important controller structures are embedded in parallel as a single package in PID controller. The structure of PID controller employed in area-1 is shown in Figure 2i. A similar PID controller is also employed in area-2. The output of PID controller in time domain is given by Eq. (5).

$$u(t) = K_p e(t) + K_i \int_0^t e(t)dt + K_d \frac{de(t)}{dt} \tag{5}$$

and it has the transfer function given by Eq. (6)

$$G(s) = K_p + \frac{K_i}{s} + K_d s, \tag{6}$$

where K_p, K_i and K_d are proportional gain, integral gain, and derivative gain of the PID controller respectively.
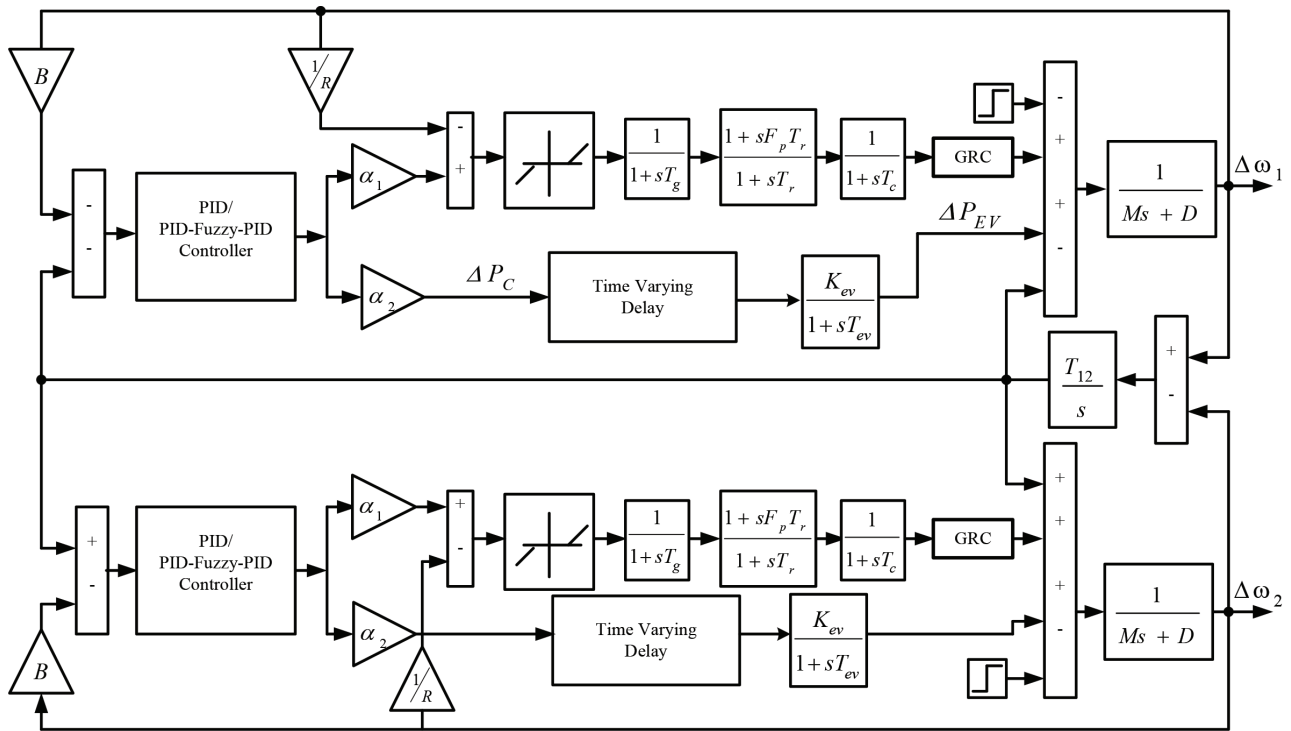
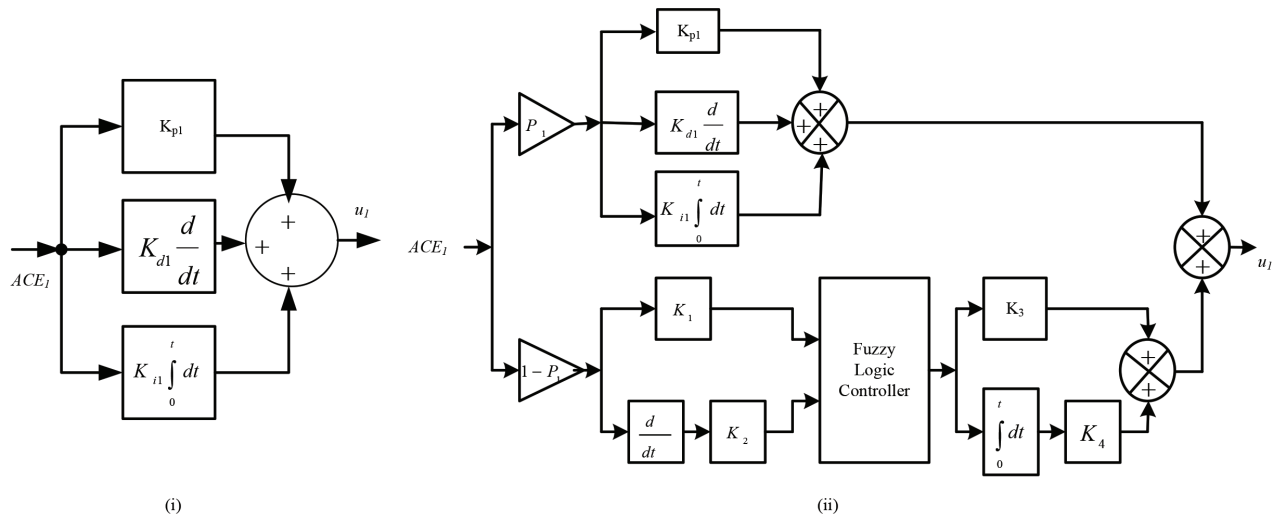Figure 1. Transfer function model of the power system under study.

(i)   (ii)

Figure 2. Structure of (i) conventional PID controller and (ii) PID-FPID controller.

3.2. PID-FPID controller

Structure of PID-FPID controller employed in area-1 is depicted in Figure 2ii. It essentially consists of a PID controller embedded in parallel with a fuzzy-PID controller. Structure of PID controller is already described in section 3.1. Fuzzy-PID controller is a combination of fuzzy-PD and fuzzy-PI controller. The important parameters of fuzzy-PID controller shown in Figure 2ii are the input scaling factors K_1, K_2 and the output scaling factors K_3, K_4. A similar PID-FPID controller is also employed in area-2 with K_5, K_6 and K_7, K_8 as

the input and output scaling factors respectively for the fuzzy-PID controller. For area-1, the ACE is multiplied by a gain P_1 to serve as the input to the PID controller and again the ACE is multiplied by a gain 1-P_1 before it is fed to the fuzzy-PID controller as shown in Figure 2ii. Similarly, for area-2, the ACE is multiplied by a gain P_2 to serve as the input to the PID controller and again the ACE is multiplied by a gain 1-P_2 before it is fed to the fuzzy-PID controller. Dynamic response of the system is determined by the controller parameters K_{p1}, K_{i1}, K_{d1}, K_{p2}, K_{i2}, K_{d2}, P_1, P_2, and K_1-K_8. Hence, these parameters must be properly tuned so as to obtain superior dynamic response.

The two inputs of the fuzzy logic controller are error and time derivative of the error. Triangular membership functions as depicted in Figure 3i are used for both the inputs as well as the output of the fuzzy logic controller. Five linguistic variables used for both the inputs as well as the output of the fuzzy logic controller are negative big (NB), negative small (NS), zero (Z), positive small (PS), and positive big (PB). Formulation of appropriate rule base is essential since it plays a vital role in determining the performance of the fuzzy logic controller. The rule base for the input and output of fuzzy logic controller is formulated by exhaustively studying the dynamic performance of the system using trial and error method and is given in Table 1. Mamdani fuzzy interface engine is chosen for this work. The centre of gravity method of defuzzification is employed in this work to determine the crisp output of the fuzzy logic controller.

Table 1. Rule base used for fuzzy logic controller.

ACE	ΔACE				
	NB	NS	Z	PS	PB
NB	NB	NB	NS	NS	Z
NS	NB	NS	NS	Z	PS
Z	NS	NS	Z	PS	PS
PS	NS	Z	PS	PS	PB
PB	Z	PS	PS	PB	PB

4. Optimal design of controllers

4.1. Objective function

Performance of any optimization method is characterized by the objective function used in the method. Hence, proper selection of objective function is vital in any optimization method. ITAE, integral absolute error (IAE), integral time square error (ITSE), and integral square error (ISE) are various objective or cost functions used to compute the system performance in time domain. ITAE-based optimization reduces the settling time as compared to IAE or ISE criterion [25]. Moreover, ITAE-based optimization has less peak overshoot. ITSE criterion has the disadvantage of giving a large controller output, if the set point changes abruptly. Hence, in this work ITAE has been taken as the objective function or cost function for tuning the controller gains. ITAE cost function is mathematically expressed as follows:

$$ITAE = \int_0^t (|\Delta\omega_1| + |\Delta\omega_2| + |\Delta P_{tie12}|)t dt, \tag{7}$$

where $\Delta\omega_1, \Delta\omega_2$ represent respectively the frequency change in area-1 and area-2, ΔP_{tie12} represents the change in power flow through tie-line, and t is the simulation time.

4.2. Optimization technique

As already stated above, the dynamic response of the system depends upon the various gains and parameters of the controller. Hence, it is essential to select these gains and parameters appropriately. Various optimization techniques have been reported in the literature for tuning the controller gains and parameters to obtain better dynamic response. In this work, the dynamic response of the system is analyzed and compared by tuning the gains of the PID controllers using PSO, SCA, MSCA, and hybrid PSO-MSCA optimization technique and parameters of PID-FPID controllers are optimized using hybrid PSO-MSCA. Various steps involved in these optimization techniques are discussed below:

4.2.1. Particle swarm optimization (PSO)

Kennedy and Eberhart were the first to introduce the particle swarm optimization method in 1995 [26]. It is one of the many population-based evolutionary algorithm used for optimization. It is inspired by simulation of social behavior based on the movements of organism in a bird flock or fish school. It is a robust method and it has the features of stable convergence, easy implementation with superior computational efficiency [27]. PSO algorithm follows the process of initialization, then evaluation and updation till maximum iteration is reached and finally selection of best solution. The steps followed in the PSO algorithm are given below.

   i. Initialization: In this stage, the initial population of size $[\text{NP} \times \text{D}]$ with initial position (X_i) and velocity (V_i) is generated, where 'NP' is the number of population and 'D' is the dimension of the search space.

   ii. Evaluation: In this stage, the power system model is run and the predefined fitness function $\text{f}(X_i)$ of each particle are evaluated and the best fitness function is selected. The corresponding solution is set as old global best $(g_{best,old})$ and the initial population (X_i) is set as old local best $(P_{best,old})$.

   iii. Updation: In this stage, the initial velocity is updated and new particles $(X_{i,new})$ are generated using the following relations:

$$V_{i,new} = w \times V_i + C_1 \times rand \times (P_{best,old} - X_i) + C_2 \times rand \times (g_{best,old} - X_i), \tag{8}$$

$$X_{i,new} = X_i + V_{i,new}, \tag{9}$$

where w is inertia weight, C_1 and C_2 are acceleration constants, and $rand$ is random number within 0 and 1. The value of C_1 and C_2 is taken as 2.05.

     Thereafter, the fitness function $\text{f}(X_{i,new})$ of each newly generated particle is evaluated and the best fitness function is selected. The corresponding solution is set as new global best $(g_{best,new})$ and the local best is updated based on the performance of $X_{i,new}$ and X_i. Based on the performance of $g_{best,new}$, g_{best} is updated and steps (ii) and (iii) are repeated till the maximum iteration is reached and finally the best solution is selected.

4.2.2. Sine cosine algorithm (SCA)

In 2016, Mirjalili [28] developed a new population-based search algorithm called sine cosine algorithm for solving optimization problems. SCA has the advantages of faster convergence and local optima avoidance. SCA sets up random candidate solutions which oscillate towards or outwards the best solution based upon a model governed by trigonometric sine and cosine functions.

Like any other population-based optimization algorithm, SCA follows the process of initialization, then evaluation and updation. The steps followed in SCA are given below.

i. Initialization: In this stage, the initial population of size $[\text{NP} \times \text{D}]$ with initial position (X_i) is generated, where 'NP' is the number of population and 'D' is the dimension of the search space.

ii. Evaluation: In this stage, the power system model is run and the predefined fitness function $\text{f}(X_i)$ of each particle is evaluated and the best fitness function is selected. The corresponding solution (P_i) is the best solution obtained so far and is assigned as target solution.

iii. Updation: In this stage, the initial position is updated using the following relation.

$$X_{i,new} = \begin{cases} X_i + r_1 \times sin(r_2) \times |r_3 P_i - X_i| & \text{if } r_4 < 0.5 \\ X_i + r_1 \times cos(r_2) \times |r_3 P_i - X_i| & \text{if } r_4 \geq 0.5 \end{cases}, \tag{10}$$

where 'P_i' is the best solution, r_2 is a random number in the range $[0,2\pi]$ and r_3 and r_4 are random numbers in the range $[0,1]$. In order to balance the exploration and exploitation to find the assured regions of search space for convergence to the global optimum, r_1 is adaptively updated by using the following equation:

$$r_1 = a - t\frac{a}{T}, \tag{11}$$

where t is the current iteration, T is the maximum number of iterations and a is a constant.

Thereafter, the fitness function $\text{f}(X_{i,new})$ of each newly generated particle is evaluated and compared with the previous one. Based on the performance of $\text{f}(X_{i,new})$, the initial position of each particle are updated and steps (ii) and (iii) are repeated till the maximum iteration is reached. Finally the best solution is retained.

There are four important parameters in SCA; r_1, r_2, r_3, and r_4. Parameter r_1 defines the area of the next position, it could be either in the space between the solution and destination or outside it. Parameter r_2 specifies the distance of movement towards or outwards the destination. Parameter r_3 holds a random weight for P_i in order to stochastically emphasize $(r_3 > 1)$ or deemphasize $(r_3 < 1)$ the effect of destination in identifying the distance. Parameter r_4 helps to switch between sine and cosine functions.

4.2.3. Modified sine cosine algorithm (MSCA)

As illustrated by the following example, SCA algorithm is modified by incorporating a mutation phase into it after updation and the new algorithm so developed is known as modified sine cosine algorithm. In mutation phase, some elements of the newly generated solution are substituted by random numbers generated in between the specified range. For instance, let the solution obtained after updation in SCA for NP = 5 and D = 6 is:

$$X_{new} = \begin{bmatrix} 0.3678 & 1.7905 & 0.1690 & 1.6765 & 1.7811 & 0.1497 \\ 1.9448 & 0.9637 & 1.3713 & 0.2708 & 1.6323 & 1.6193 \\ 0.9150 & 1.6874 & 1.0495 & 0.6873 & 1.8255 & 0.3012 \\ 1.9948 & 1.1153 & 0.7307 & 1.5211 & 1.1695 & 1.3043 \\ 1.5333 & 1.5800 & 0.4880 & 1.7630 & 0.3971 & 0.4026 \end{bmatrix} \tag{12}$$

In order to incorporate the mutation phase, five random integers are generated within the range [1,6]. Let the random integers generated are given by:

$$R_i = \begin{bmatrix} 6 & 2 & 4 & 5 & 3 \end{bmatrix}. \tag{13}$$

Hence, in the mutation phase, 6th element of 1st population (1st row of X_{new}), 2nd element of 2nd population, 4th element of 3rd population and so on are substituted by random numbers generated in between a specified range of the variables i.e. [0,2]. Let the random numbers so generated be:

$$R_4 = \begin{bmatrix} 0.2587 & 1.4128 & 1.1034 & 1.6871 & 1.9533 \end{bmatrix}. \tag{14}$$

After substitution, the new solution becomes as given below.

$$X_{new1} = \begin{bmatrix} 0.3678 & 1.7905 & 0.1690 & 1.6765 & 1.7811 & \mathbf{0.2587} \\ 1.9448 & \mathbf{1.4128} & 1.3713 & 0.2708 & 1.6323 & 1.6193 \\ 0.9150 & 1.6874 & 1.0495 & \mathbf{1.1034} & 1.8255 & 0.3012 \\ 1.9948 & 1.1153 & 0.7307 & 1.5211 & \mathbf{1.6871} & 1.3043 \\ 1.5333 & 1.5800 & \mathbf{1.9533} & 1.7630 & 0.3971 & 0.4026 \end{bmatrix} \tag{15}$$

Finally, the fitness values of both the solution X_{new} and X_{new1} are evaluated and the best performing solutions are selected for the next iteration. For instance, if the fitness values are:

$$For\, X_{new};\, fit_1 = \begin{bmatrix} 0.6963 & 0.4434 & 0.4708 & 0.0125 & 0.4078 \end{bmatrix}, \tag{16}$$

$$For\, X_{new1};\, fit_2 = \begin{bmatrix} 0.6356 & 0.4950 & 0.1152 & 0.5095 & 0.4931 \end{bmatrix}, \tag{17}$$

then 1st and 3rd solutions are to be taken from X_{new1} and rest of the solutions from X_{new}. Thus, the solution that will participate in next iteration is given by:

$$X_{new1} = \begin{bmatrix} 0.3678 & 1.7905 & 0.1690 & 1.6765 & 1.7811 & \mathbf{0.2587} \\ 1.9448 & 0.9637 & 1.3713 & 0.2708 & 1.6323 & 1.6193 \\ 0.9150 & 1.6874 & 1.0495 & \mathbf{1.1034} & 1.8255 & 0.3012 \\ 1.9948 & 1.1153 & 0.7307 & 1.5211 & 1.1695 & 1.3043 \\ 1.5333 & 1.5800 & 0.4880 & 1.7630 & 0.3971 & 0.4026 \end{bmatrix}. \tag{18}$$

4.2.4. Hybrid PSO-MSCA

The advantage of MSCA is its capability to keep diversity in population to explore the local search, whereas its main disadvantage is nonexistence of memory, which may lead the solution to stick in local optima. PSO integrates individual cognition (P_{best}) and social collaboration (g_{best}). However, the lack of diversity in swarm in PSO algorithm may show instability in few solutions and may get trapped in local optima. Therefore, in this article to maintain the diversity and to add memory in population, hybrid PSO-MSCA is suggested to optimally design the proposed control approach. Steps involved in this hybridization process are as follows:

i. Initialization: In this step an initial population 'X_i' of size [NP×D] is randomly generated. Each solution of the population is evaluated and the best performing solution is considered as 'g_{best}' and the initial population is taken as 'P_{best}'. Then an initial velocity vector 'V_i' of size same as initial population is randomly generated.

PSO algorithm begins here

ii. Velocity and population updation: Here the initial velocity 'V_i' and initial population 'X_i' are updated using Eqs. (8) and (9) respectively. The updated velocity is 'V_{new}' and updated population is 'X_{new}'.

iii. Evaluation of updated population: In this phase the updated population is evaluated and finest solution is considered as '$g_{best,new}$'. If $g_{best,new}$ performs better than g_{best}, then $g_{best,new}$ is considered the global solution and vice versa. Local best solution '$P_{best,new}$' is generated by selecting the best-performing solution among 'X_i' and 'X_{new}'.

PSO algorithm ends here and MSCA begins here

iv. Solution updation: Solution obtained from the last step of PSO algorithm '$X_{pbest,new}$' is taken as initial solution for MSCA and is updated to generate new set of solution 'X_{new1}' using Eq. (10). Updated population is evaluated and again modified to obtain 'X_{new2}' using Eqs. (12–18) clearly explained in modification stage of SCA in Section 4.2.3.

v. Evaluation of updated population: In this phase updated solutions 'X_{new1}' and 'X_{new2}' are evaluated, the best-performing one is considered '$g_{best,new1}$' and the best solution from 'X_{new1}' and 'X_{new2}' are stored in 'X_{new3}'. This newly generated solution 'X_{new3}' is taken as initial population of the PSO algorithm in step (ii).

MSCA ends here

vi. Steps (ii)–(v) are repeated until stopping criterion is met.

5. Result analysis

5.1. Transient response analysis

Dynamic performance of the designed two-equal-area interconnected nonlinear reheat thermal power system incorporating EV aggregator with time-varying delay in each area for AGC is investigated in MATLAB Simulink environment by applying a step load perturbation of 10 % in area-1. The investigation is carried out using two controllers namely PID and PID-FPID. Four different optimization techniques: PSO, SCA, MSCA, and hybrid PSO-MSCA are used to tune the gains of the PID controller and hybrid PSO-MSCA is used to tune the different parameters of the proposed PID-FPID controller. Furthermore, a base case scenario has been taken to examine the effectiveness of the recommended control strategy and for the same, the power system model is equipped with an integral controller tuned by PSO algorithm. Thus, the dynamic performance of the system under study is investigated for six different cases: a base case with PSO-based integral controller, four cases using PID controller tuned through PSO, SCA, MSCA, PSO-MSCA, and one case using PID-FPID controller tuned through hybrid PSO-MSCA. Optimal gains of the controllers and values of the objective function (ITAE) with different controllers for a simulation time of 70 s are depicted in Tables 2 and 3. From Tables 2 and 3, it is clear that minimum value of the objective function (ITAE) is obtained with the suggested control approach.

Frequency oscillations in area-1 and area-2 are shown in Figures 3ii and Figure 4i respectively and tie-line power oscillation is shown in Figure 4ii. Dynamic performance of the AGC system with I/PID/PID-FPID controllers tuned through various optimization techniques in terms of undershoot (U_{sh}), overshoot (O_{sh}), and settling time (T_s) of frequency deviation in area-1 (Δf_1) and in area-2 (Δf_2) and tie-line power deviation (ΔP_{tie}) are depicted in Table 4. It is found from Figures 3ii, 4i, 4ii and Table 4 that the PID controllers designed with different optimization techniques are performing better in comparison to the PSO optimized integral controller and further it is observed that hybrid PSO-MSCA–based PID controller delivers supreme response as compared to other PID controllers. In addition, it is evident that the overall transient performance

of AGC system with PID-FPID controller tuned by hybrid PSO-MSCA is superior to the PSO, SCA, MSCA, hybrid PSO-MSCA optimized PID controllers.
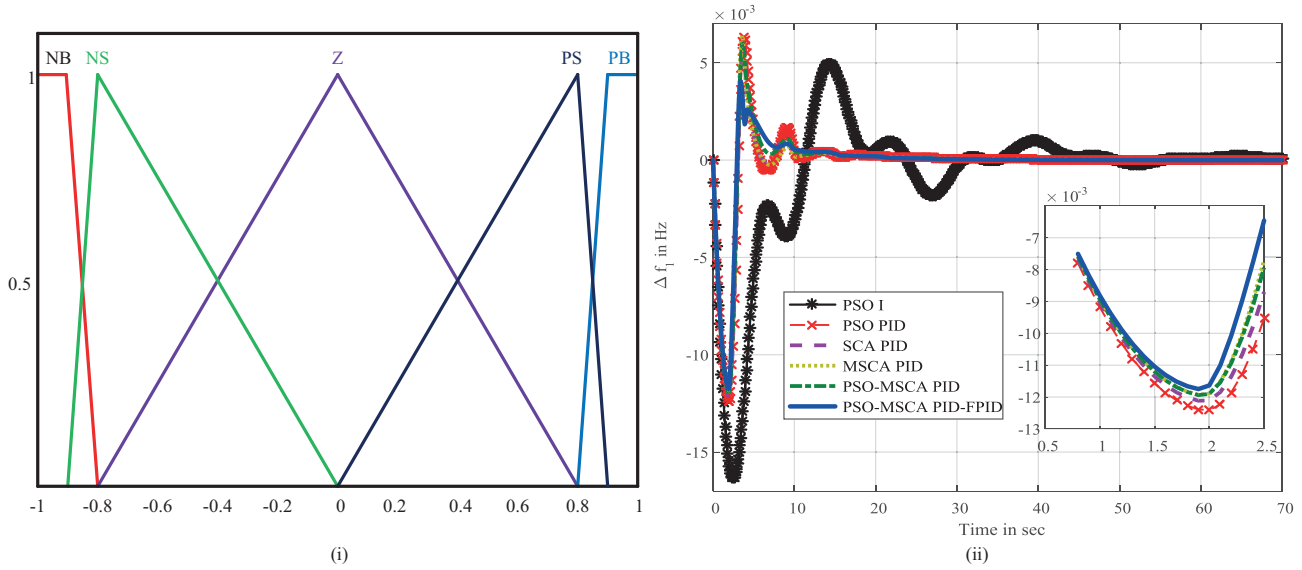

Figure 3. (i)Fuzzy membership function structure and (ii) frequency deviation in area-1.
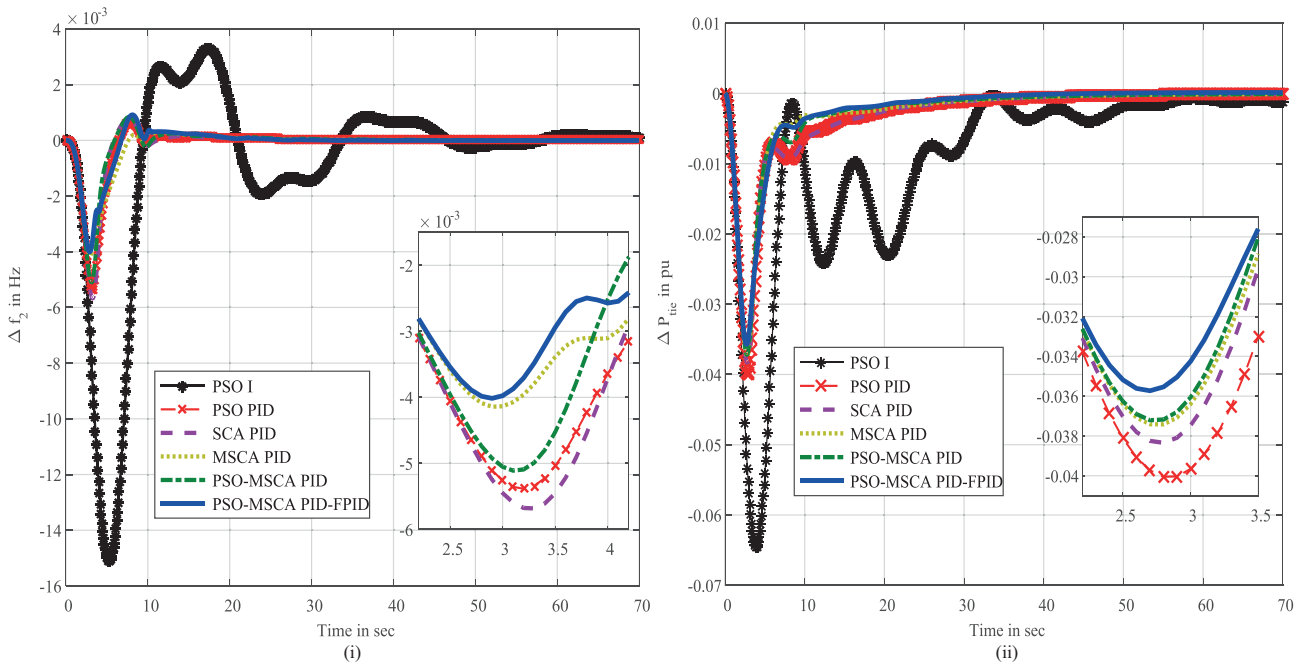

Figure 4. (i)Frequency deviation in area-2 and (ii) tie-line power deviation.

Frequency deviation in area-1(Δf_1) in terms of undershoot, overshoot, and settling time in case of PID-FPID controller tuned with PSO-MSCA is less as compared to PSO, SCA, MSCA, and hybrid PSO-MSCA tuned PID controller. For the frequency deviation in area-2(Δf_2), PSO-MSCA-based PID-FPID controller gives the least undershoot while MSCA-based PID controller gives the least overshoot, and SCA-based PID

Table 2. Optimal gains of of I/PID controllers with ITAE values.

Controllers	Controller gains of area-1			Controller gains of area-2			ITAE
	K_{p1}	K_{i1}	K_{d1}	K_{p2}	K_{i2}	K_{d2}	
PSO I	NA	0.0773	NA	NA	0.0100	NA	13.3302
PSO PID	1.8704	0.4346	0.2988	1.5054	0.0100	0.5425	2.5505
SCA PID	2.0000	0.4586	0.4930	1.5327	0.0139	0.0100	2.5405
MSCA PID	2.2832	0.4698	0.7589	1.2176	0.0100	2.2994	2.1617
Hybrid PSO-MSCA PID	2.0000	0.5859	0.7489	2.000	0.0100	0.1990	2.0123

Table 3. Optimal gains of PSO-MSCA tuned PID-FPID controller with ITAE value.

Gains of area-1								ITAE
K_{p1}	K_{i1}	K_{d1}	P_1	K_1	K_2	K_3	K_4	
2.0000	0.6625	1.6013	0.9500	1.1557	0.8967	0.2146	1.1600	
Gains of area-2								1.6501
K_{p2}	K_{i2}	K_{d2}	P_2	K_5	K_6	K_7	K_8	
2.0000	0.1000	2.0000	0.9500	1.1429	0.9623	1.1189	0.6928	

Table 4. Transient performance analysis of various controllers.

Controllers	Δf_1			Δf_2			ΔP_{tie}		
	U_{sh} $\times 10^{-3}$	O_{sh} $\times 10^{-3}$	T_s	U_{sh} $\times 10^{-3}$	O_{sh} $\times 10^{-3}$	T_s	U_{sh} $\times 10^{-3}$	O_{sh} $\times 10^{-3}$	T_s
PSO I	-16.3159	4.9411	52.7000	-15.1267	3.2898	50.9	-64.6629	0	49.6000
PSO PID	-12.4373	6.3857	20.3088	-5.4035	0.6718	8.8433	-40.0505	0	21.3609
SCA PID	-12.1653	6.1656	20.1477	-5.7208	0.8222	8.8009	-38.4023	0	21.4402
MSCA PID	-11.9493	6.5469	19.3164	-4.1721	0.3252	16.1346	-37.3974	0	20.8479
PSO-MSCA PID	-11.9636	6.1966	19.6134	-5.1322	0.8404	14.3007	-37.2001	0	17.9014
PSO-MSCA PID-FPID	-11.7678	4.3029	17.94	-4.0265	0.8947	16.4796	-35.6384	0	16.4796
PSO-MSCA PID-FPID with 2EVs in each area	-11.8141	16.5464	16.2000	-4.0717	0.67313	66.9000	-33.1909	0.5751	16.0000
PSO-MSCA PID-FPID with SLP 0.4 pu	-63.5775	12.9369	56.0000	-24.4447	1.7373	33.8	-195.7128	19.18	73.2

controller has the least settling time. The increase in peak overshoot in case of PSO-MSCA based PID-FPID controller as compared to MSCA-based PID controller having least overshoot is 0.0005695 Hz and similarly the increase in settling time in case of PSO-MSCA–based PID-FPID controller as compared to SCA-based PID controller having least settling time is 7.6787 s. Hence, there is no appreciable increase in peak overshoot and settling time of frequency deviation in area-2 (Δf_2) with PSO-MSCA–based PID-FPID controller. Taking Ptie
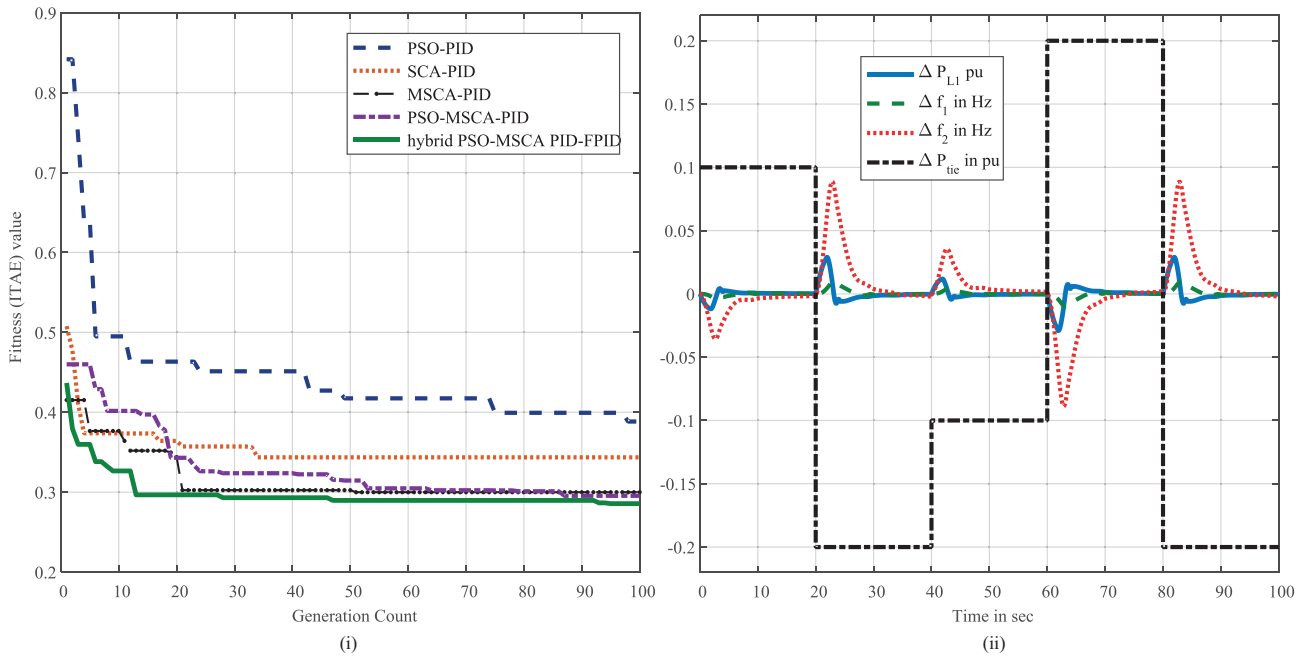
Figure 5. (i)Convergence Profile and (ii)Random loading and corresponding response.

into consideration, PSO-MSCA–based PID-FPID controller has the least peak undershoot and settling time as compared to PSO-, SCA-, PSO-MSCA, and MSCA-based PID controller.

From the above analysis, it is clear that PSO-MSCA–based PID-FPID controller has the better dynamic performance as far as response of frequency deviation in area-1 (Δf_1) and tie-line power deviation (ΔP_{tie}) is concerned. In view of this and keeping in mind the system complexity arising due to time-varying delay characteristics of EV aggregator, the small increase in peak overshoot and settling time of the frequency deviation in area-2 (Δf_2) with PSO-MSCA–based PID-FPID controller is well within the limits and acceptable. Hence, the overall dynamic performance of PSO-MSCA–based PID-FPID controller is considered to be superior in comparison with the PSO-, SCA-, PSO-MSCA-, MSCA-based PID controller. Moreover, the PSO-MSCA-based PID-FPID controller has the fastest convergence towards the optimal solution as shown in Figure 5i.

5.2. Robustness analysis

Robustness of the recommended PSO-MSCA–optimized PID controller is verified by considering three cases: (i) incorporating two EV aggregators with time-varying delay in each area with 0.2 participation ratio each, (ii) applying a large disturbance of 0.4 p.u. in area-1, and (iii) applying a random load in area-1. The transient response parameters for Cases (i) and (ii) are recorded in Table 4 which shows that the recommended control approach has the ability to damp out the oscillation and retain the system stability in these conditions as well. For Case (iii), nature of random load and the corresponding system response is depicted in Figure 5ii. It is witnessed from Figure 5ii that the suggested control approach is able to maintain the system stability with this condition as well. Hence, it is proved that the proposed control approach is quite robust.

6. Conclusion

In this work, a novel effort has been made to study the dynamic performance of AGC system incorporating EV aggregators with time delay characteristics using different controllers with various optimization techniques. For

this purpose, a two-area interconnected nonlinear reheat type thermal power system having an EV aggregator with time-varying delay in each area is considered. Two independent controllers, PID and PID-FPID, are used to study the dynamic performance of the system. First, the dynamic performance of the system is investigated with PID controllers, independently using PSO, SCA, MSCA, and hybrid PSO-MSCA as optimization techniques to tune the gains of the controller. Then, PID-FPID controller with hybrid PSO-MSCA as the optimization technique is used to study the dynamic performance of the system. A step load perturbation of 10% in area-1 is applied in each case. After analyzing all the prospects of dynamic performance of the system and recognizing the system complexity as a consequence of time-varying delay characteristics of EV aggregator, it is considered that the overall dynamic performance of PSO-MSCA–based PID-FPID controller is superior to the PSO-, SCA-, PSO-MSCA-, and MSCA-based PID controller. Furthermore, the proposed control strategy has the best convergence profile amongst all. Robustness analysis was carried out to validate the robustness of the recommended control strategy by (i) incorporating two EV aggregators with time-varying delay in each area, (ii) applying a large disturbance of 0.4 p.u. in area-1, and (iii) applying a random load in area-1. It was observed that in all the cases the controller is able to retain the system stability.

Appendix

Power system parameters taken in this study.

$M = 8.8$; $D = 1$; $T_g = 0.2$; $T_c = 0.3$; $T_r = 12$; $F_p = 1/6$; $R = 1/11$; $B = 21$; $K_{ev} = 1$; $T_{ev} = 0.1$; $\alpha_1 = 0.6$; $\alpha_2 = 0.4$; $T_{12} = 2$.

<div align="center">

References

</div>

[1] Kempton W, Letendre SE. Electric vehicles as a new power source for electric utilities. Transportation Research Part D: Transport and Environment 1997; 2 (3): 157-175.

[2] Lopes JAP, Almeida PMR, Soares FJ. Using vehicle-to-grid to maximize the integration of intermittent renewable energy resources in islanded electric grids. In: IEEE 2009 International Conference on Clean Electrical Power; Capri, Italy; 2009. pp. 290-295.

[3] Brooks AN. Vehicle-to-grid demonstration project: Grid regulation ancillary service with a battery electric vehicle. Sacramento, CA, USA: California Environmental Protection Agency, Air Resources Board, Research Division: 2002.

[4] Liu H, Hu Z, Song Y, Lin J. Decentralized vehicle-to-grid control for primary frequency regulation considering charging demands. IEEE Transactions on Power Systems 2013; 28 (3): 3480-3489.

[5] Masuta T, Yokoyama A. Supplementary load frequency control by use of a number of both electric vehicles and heat pump water heaters. IEEE Transactions on Smart Grid 2012; 3 (3): 1253-1262.

[6] Sortomme E, El-Sharkawi MA. Optimal charging strategies for unidirectional vehicle-to-grid. IEEE Transactions on Smart Grid 2011; 2 (1): 131-138.

[7] Sortomme E, El-Sharkawi MA. Optimal scheduling of vehicle-to-grid energy and ancillary services. IEEE Transactions on Smart Grid 2012; 3 (1): 351-359.

[8] Sortomme E, El-Sharkawi MA. Optimal combined bidding of vehicle-to-grid ancillary services. IEEE Transactions on Smart Grid 2012; 3 (1): 70-79.

[9] Han S, Han S, Sezaki K. Development of an optimal vehicle-to-grid aggregator for frequency regulation. IEEE Transactions on smart grid 2010; 1 (1): 65-72.

[10] Lopes JAP, Soares FJ, Almeida PM. Integration of electric vehicles in the electric power system. Proceedings of the IEEE 2011; 99 (1): 168-183.

[11] Kempton W, Udo V, Huber K, Komara K, Letendre S et al. A test of vehicle-to-grid (V2G) for energy storage and frequency regulation in the PJM system. Results from an Industry-University Research Partnership, University of Delaware, Newark, DE, US: 2008.

[12] Bessa RJ, Matos MA. The role of an aggregator agent for EV in the electrical market. In: 2010 Mediterranean Conference and Exhibition on Power Generation, Transmission, Distribution and Energy Conversion (MedPower 2010); Agia Napa, Cyprus; 2010. pp. 1-9.

[13] Zhang CK, Jiang L, Wu QH, He Y, Wu M. Delay-dependent robust load frequency control for time delay power systems. IEEE Transactions on Power Systems 2013; 28 (3): 2192-2201.

[14] SÖNMEZ Ş, Ayasun S, EMİNOĞLU U. Computation of time delay margins for stability of a single-area load frequency control system with communication delays. WSEAS Transactions on Power Systems 2014; 9: 67:76.

[15] Macana CA, Mojica-Nava E, Quijano N. Time-delay effect on load frequency control for microgrids. In: IEEE 2013 International Conference on Networking, Sensing and Control; Evry, France; 2013. pp. 544-549.

[16] Ko KS, Sung DK. The effect of EV aggregators with time-varying delays on the stability of a load frequency control system. IEEE Transactions on Power Systems 2018; 33 (1): 669-680.

[17] Liu S, Wang X, Liu PX. Impact of communication delays on secondary frequency control in an islanded microgrid. IEEE Transactions on Industrial Electronics 2015; 62 (4): 2021-2031.

[18] Wen S, Yu X, Zeng Z, Wang J. Event-triggering load frequency control for multiarea power systems with communication delays. IEEE Transactions on Industrial Electronics 2016; 63 (2): 1308-1317.

[19] Kottick D, Blau M, Edelstein D. Battery energy storage for frequency regulation in an island power system. IEEE Transactions on Energy Conversion 1993; 8 (3): 455-459.

[20] Lee DJ, Wang L. Small-signal stability analysis of an autonomous hybrid renewable energy power generation/energy storage system part I: Time-domain simulations. IEEE Transactions on Energy Conversion 2008; 23 (1): 311-320.

[21] Khayyer P, Ozguner U. Decentralized control of large-scale storage-based renewable energy systems. IEEE Transactions on Smart Grid 2014; 5 (3): 1300-1307.

[22] Richard JP. Linear time delay systems: Some recent advances and open problems. IFAC Proceedings Volumes 2000; 33 (23): 5-19.

[23] Jeung ET, Kim JH, Park HB. Robust controller design for uncertain systems with time delays: LMI approach. Automatica 1996; 32 (8): 1229-1231.

[24] Ikeda M, Ashida T. Stabilization of linear systems with time-varying delay. IEEE Transactions on Automatic Control 1979; 24 (2): 369-370.

[25] Lee CH, Chang FK. Fractional-order PID controller optimization via improved electromagnetism-like algorithm. Expert Systems with Applications 2010; 37 (12): 8871-8878.

[26] Kennedy J, Eberhart R. Particle Swarm Optimization (PSO). In: 1995 Proceedings IEEE International Conference on Neural Networks; Perth, Australia; 1995. pp. 1942-1948.

[27] Eberhart RC, Shi Y. Comparison between genetic algorithms and particle swarm optimization. In: Springer 1998 International Conference on Evolutionary Programming; Berlin, Heidelberg; 1998. pp. 611-616.

[28] Mirjalili S. SCA: a sine cosine algorithm for solving optimization problems. Knowledge-Based Systems 2016; 96: 120-133.